IEICE Proceeding Series

Deterministic polarization chaos in a laser diode

Marc Sciamanna, Martin Virte, Hugo Thienpont, Krassimir Panajotov

Vol. 1 pp. 195-198
Publication Date: 2014/03/17
Online ISSN: 2188-5079

2012 International Symposium on Nonlinear Theory and its Applications
NOLTA2012, Palma, Majorca, Spain, October 22-26, 2012

Deterministic polarization chaos in a laser diode

Marc Sciamanna‡, Martin Virte†,‡, Hugo Thienpont‡ and Krassimir Panajotov‡

†Supélec, OPTEL Research Group, Laboratoire Matériaux Optiques, Photonique et Systèmes (LMOPS) EA-4423,
2 Rue Edouard Belin, F-57070 Metz, France
‡Department of Applied Physics and Photonics (IR-TONA), Vrije Universiteit Brussels,
Pleinlaan 2, 1050 Brussels, Belgium
Email: marc.sciamanna@supelec.fr

Abstract—Experiments on quantum well and recently quantum dot VCSELs have shown that the increase of injection current may lead to a transition from a linearly polarized light emission at threshold to a region of nonlinear dynamics (self-pulsing) accompanying polarization switching. However these experiments brought different conclusions on the frequency of self-pulsation: the polarization dynamics occurred on a nanosecond time-scale that related either to the birefringence induced frequency splitting or to the relaxation oscillation frequency. With the use of advanced continuation methods applied to the well-known spin-flip (SFM) model, we bring now new light into the bifurcations explaining deterministic self-pulsing and deterministic polarization chaos. We are then able not only to reconcile these a priori contradicting experiments and to interpret experimental results as resulting from polarization chaos.

1. Introduction

Vertical-cavity surface-emitting lasers (VCSELs) are today replacing conventional Edge-emitting lasers (EELs) in numerous applications. However in these structures the polarization selection is much weaker than in EELs, and in many experiments one typically observes polarization instabilities and even a particularly striking feature called polarization switching (PS) [1]. Although a VCSEL generally starts emitting in a linearly polarized (LP) mode, an increase of the injection current can induce a switching to the orthogonal LP mode. As a result of cavity birefringence these two modes are frequency detuned, we refer to them as the low (LF) and high (HF) frequency linear polarization. A switching from HF to LF (resp. LF to HF) is identified as a type I PS (resp. type II PS). Typically PS is accompanied by noise driven bistable mode hopping [2], but two experiments have shown more complex dynamical transition accompanying PSs. In these cases, the increase of current leads to elliptically polarized states and complex dynamical self-pulsing occurring at nanosecond time-scale [3, 4]. The frequency of these dynamics relate either to the birefringence induced frequency [3] or to the relaxation oscillation frequency [4]. The bifurcations underlying these dynamical transitions and what determines the frequencies of the self-pulsing dynamics remain issues to be clarified.

A dynamical approach of these polarization instabilities in VCSEL has been proposed by San Miguel et al[5], the so-called San Miguel-Feng-Moloney (SFM) or spin-flip model. A four-level model is considered, accounting for two separated processes for the left (-) and right (+) circularly polarized emission with two separated carrier reservoir but coupled through the complex spin-flip processes equilibrating the carrier population. The SFM steady-states have been extensively studied by means of asymptotic methods or direct numerical integration [6, 7] and it appears that SFM allows for linearly and elliptically polarized states. The stability analysis of these steady-states revealed that both type I and type II PSs are possible in the framework of SFM. Despite these analysis, there is, to our best knowledge, no investigation of the higher order bifurcations that may lead to complex nonlinear dynamics. In particular there is no study of the frequencies of the polarization dynamics and how they may depend on the laser parameters.

In this contribution, by means of direct numerical integration and advanced continuation techniques, we provide a valuable insight of the bifurcation scenarios leading to complex nonlinear dynamics in the framework of SFM. Continuation techniques allow to follow numerical solution in the phase-space regardless of their stability and therefore to reveal the underlying mechanism and bifurcation sequences creating the dynamical states. Of particular interest is the Hopf bifurcations analysis which gives the fundamental frequency of the emerging periodic solution. Therefore we make an in-depth bifurcation analysis of the scenario leading to self-pulsating dynamics and we demonstrate that the frequency of these dynamics is in fact a bifurcation problem: depending on the parameters, the frequency can be either close to the birefringence induced frequency or to the relaxation oscillation frequency. Thus our work reconciles both experiments [3, 4] but also brings new details to our theoretical understanding of SFM.

2. Rate equation of the system: The San Miguel-Feng-Moloney approach

The San Miguel-Feng-Moloney model (SFM) or spin-flip model described by San Miguel et al [5], considers two slowly varying enveloppes for the left $E_- = R_- e^{i\psi_-}$ and

right $E_+ = R_+ e^{i\psi_+}$ circularly polarized emissions with two distinct carrier populations D_- and D_+. Yet the population carrier is described by $N = D_+ + D_-$ the total carrier population and $n = D_+ - D_-$ the population difference. For simplicity and to allow for a numerical treatment, we consider the phase difference $\Phi = \psi_+ - \psi_-$, see [6]. The SFM equation set can be written as follows:

$$\frac{dR_\pm}{dt} = \kappa(N + n - 1)R_\pm - (\gamma_a cos(\Phi) \pm \gamma_p sin(\Phi))R_\mp \quad (1)$$

$$\frac{d\Phi}{dt} = 2\kappa\alpha n - (\frac{R_-}{R_+} - \frac{R_+}{R_-})\gamma_p cos(\Phi) \quad (2)$$

$$+(\frac{R_+}{R_-} + \frac{R_+}{R_-})\gamma_a sin(\Phi) \quad (3)$$

$$\frac{dN}{dt} = -\gamma[N - \mu + (N + n)R_+^2 + (N - n)R_-^2] \quad (4)$$

$$\frac{dn}{dt} = -\gamma_s n - \gamma[(N + n)R_+^2 - (N - n)R_-^2] \quad (5)$$

κ is the decay rate of the electric field in the cavity, α is the linewidth enhancement factor, μ is the normalized injection current. γ is the decay rate of the total carrier number and γ_s is the decay rate of the spin-flip relaxation processes that equilibrates the spin orientation of both carrier reservoirs. The phase and amplitude anisotropies are noted γ_p and γ_a. We applied a chosen frequency shift of $\omega_0 = \kappa\alpha$ to the original set of equation which lead to a zero emission frequency for $E_\pm$ at threshold for $\gamma_a = 0$ and $\gamma_p = 0$; thus ω_0 is our reference frequency. In this contribution, unless stated otherwise, we will use the following parameter values: $\gamma_a = -0.7\ ns^{-1}$, $\gamma_s = 100\ ns^{-1}$, $\gamma = 1$, $\kappa = 600\ ns^{-1}$, $\alpha = 3$. The system is symmetric in terms of birefringence γ_p for the right and left circularly polarized light emissions, hence we will only use $\gamma_p > 0$.

3. Nonlinear dynamics in a type II polarization switching

In this section we first investigate the nonlinear dynamics that accompanies a type II polarization switching, i.e. a configuration similar to the experiment of Ref. [3]. We use the following parameters $\gamma_a = -0.7$ and $\gamma_p = 4$, and we find a complete scenario of type II switching by varying the normalized injection current in $\mu \in [1,\ 2]$. Figure 1 shows a bifurcation diagram obtained by continuation of the SFM equations, with the use of the Matlab package DDE-BIFTOOL. We plot in panel (a) the maximum and minimum of $A = R_+^2/(\mu - 1)$ versus the normalized injection current μ. Although the representation of figure 1-(a) seems complex, the two linearly polarized states correspond to the same line $A = 1/2$ (but with different phases) which allow us to identify easily the other polarization states.In figure 1-(b) we plot the frequency of the periodic solutions versus the current μ; we also add the birefringence induced splitting frequency F_{split} (black dashed curve) and the relaxation oscillation frequency F_{RO} (red dashed curve). The panel (b) therefore will tell us more about the frequency

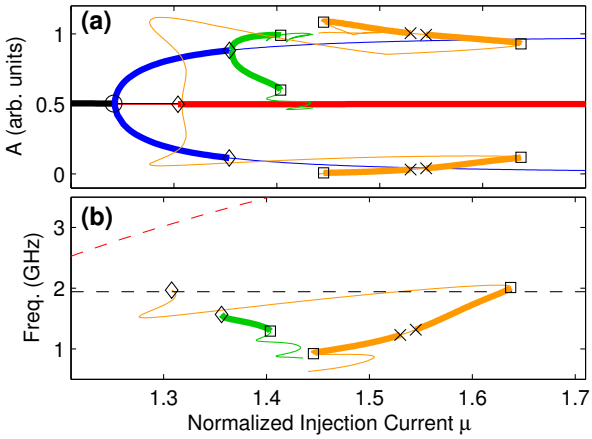

Figure 1: (color online) Continuation results for a type II switching. the stable (unstable) part of the branches are in thick (thin) lines. (a) Maximum and minimum of $A = R_+^2/(\mu - 1)$ versus normalized injection current (b) Frequency of the periodic solutions versus normalized injection current. The X and Y-LPs are in black and red respectively and the EP states are in blue. The periodic solution created on the EP states is in green (a similar branch is created at the lower hopf bifurcation but not represented) while the one created on the Y-LP state is in orange. Diamonds are hopf, squares are saddle-node and crosses are period doubling bifurcations. On diagram (b) the black dashed line gives F_{split} and the red one F_{RO} which is not displayed for $\mu > 1.4$.

of the emerging self-pulsating dynamics and further secondary bifurcations, hence comparing with the conclusions from the two experiments [3, 4].

To illustrate the observed nonlinear dynamics, we show in figure 2 Fast Fourrier Transform (FFT) optical spectra, phase space projection in the plane $(Re(E_X),\ Re(E_Y))$ and intensity time-traces for samples at six different currents.

The laser starts emitting in X-LP state with $E_y = 0$, since the choice of the parameters leads to a smaller lasing threshold for the X-LP than for the Y-LP mode. As shown in figure 2-(a.1) the lasing frequency is slightly lower than ω_0 and the laser emits in the LF mode. At $\mu = 1.24$ the steady-state is destabilized by a pitchfork bifurcation, which can be clearly identified on figure 1, creating the two EP states. Figures 2-(b.1) and (b.2) show an elliptically polarized lasing mode with locking of the frequencies of the X- and Y-polarized modes. When increasing the injection current further and starting from $\mu = 1.36$, the EP states are both destabilized by a Hopf bifurcation creating two symmetrical limit cycles leading the system to a time-periodic self-pulsation (diamond symbol in figure 1). Both EP are given (blue line) but only one periodic solution emerging from the Hopf bifurcation on the EP branch is displayed (green line). According to the continu-

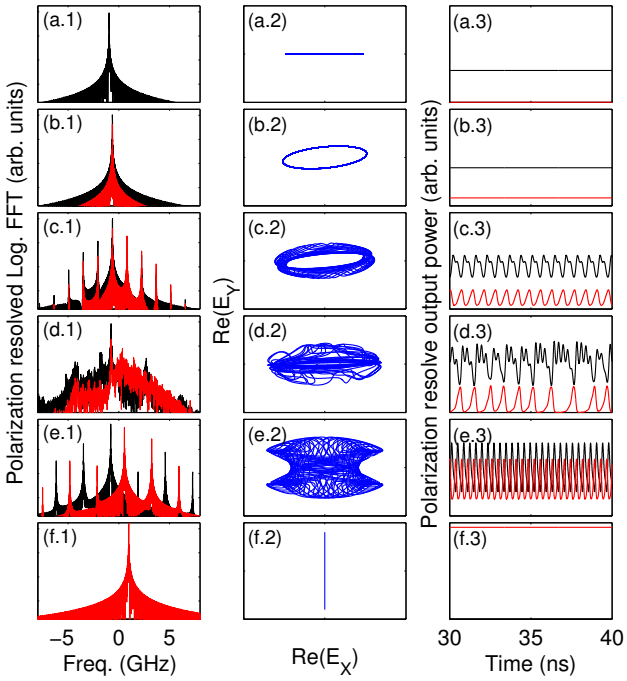

Figure 2: color online) Detailed characteristic of dynamical states for (a) $\mu = 1.223$, (b) $\mu = 1.323$, (c) $\mu = 1.381$, (d) $\mu = 1.416$, (e) $\mu = 1.549$ and (f) $\mu = 1.650$. Left: optical spectrum, Middle: phase space projection in $(Re(E_X),\ Re(E_Y))$ plane, Right: polarization-resolved time. Red (black) is for the X (Y) linear polarization axis.

ation results of figure 1 (b) the frequency of the emerging time-periodic dynamics is about 1.5 GHz which is close to F_{split} and clearly less than F_{RO} ($\sim$ 3 GHz in this injection current range). The limit cycle dynamics born on the EP solutions gets destabilized by a saddle-node bifurcation on limit cycle for a larger value of the injection current: $\mu = 1.404$ (square symbol in figure 1). Figure 2 (c.1)-(c.3) shows an example of such limit cycle dynamics with an optical spectrum being centered at ω_0 and with side-bands at harmonics of the fundamental frequency ($\sim F_{split}$). The time-traces of the X- and Y-LP mode dynamics show anti-correlated dynamics of square-like waveforms. For a current value larger than the saddle-node bifurcation on limit cycle, the laser exhibits a chaotic dynamics that coexists with a stable steady-state solution with Y-linear polarization. The region of chaos extends up to $\mu \sim 1.47$, which corresponds to a saddle-node bifurcation on a time-periodic solution emerging from a subcritical Hopf bifurcation on the Y-LP mode (Hopf: diamond symbol on the red branch and saddle-node: square symbol on the orange branch in figure 1). The optical spectrum for the chaotic time-series is given in figure 2-(d.1) and it shows a broad spectrum with however spectral signatures at frequencies close to the one of now unstable limit cycle dynamics (green thin line on figure 1 around 1 GHz) and close to F_{RO}. The polarization resolved time-series of figure 2-(c.3) and (d.3) are strongly anti-correlated. As mentioned earlier, when increasing the current above $\mu = 1.47$ the system reaches a new periodic solution born on the Y-LP steady-state branch from a subcritical Hopf bifurcation. An example of such dynamics is shown in Figure 2-(e.1) and (e.3). The laser exhibits a two mode self-pulsating dynamics. The optical spectra of the X and Y-LP modes show different central frequencies being separated by F_{split} and with side-bands at frequencies being multiples of the frequency of the limit cycle dynamics, as determined by the continuation method (orange curve in figure 1). Interestingly, the polarization resolved time-series are not anticorrelated anymore, but the modes emit pulses in phase, see figure 2-(e.3). This limit cycle dynamics is stable up to a current value of about $\mu = 1.638$, which corresponds to a second saddle-node bifurcation on the limit cycle solution. For larger current values the laser is left with a single attractor being a steady-state dynamics with Y-linear polarization, see Figure 2-(f.1)-(f.3).

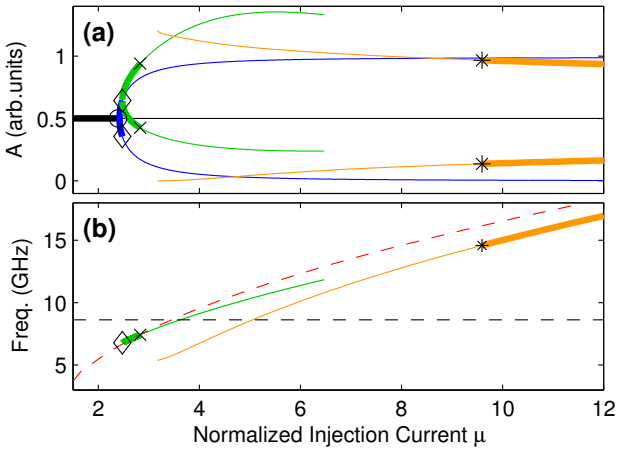

Figure 3: (color online) Continuation results for $\gamma_a = -0.7$ and $\gamma_p = 25$: the stable (unstable) part of the branches are in thick (thin) lines. The caption is similar to the one of figure 1. We find a large region without any stable states and where the laser exhibits complex nonlinear dynamics.

4. Nonlinear dynamics without polarization switching

In the previous section we made a detail analysis of a type II PS which is in good qualitative agreement with the experiment of Sondermann et al[3]. Experimentally the laser was found to go from the low to the high frequency state through a complex and dynamical transition: 1/ experiencing an elliptically polarized state, 2/ exhibiting self-pulsating dynamics at the birefringence induced frequency, 3/ emitting with a broad optical spectrum with two main peaks and multiple sidebands. In addition the reported experimental time-traces are close to the one described in figure 2-(d.3) even if correlation and DC-information are not available in the reported observations.

In this section we simulate another configuration similar to the experimental report of Olejniczak et al[4] describing a destabilization of the linearly polarized state without polarization switching; in particular a self-pulsing dynamic at the relaxation oscillation frequency is reported.

This situation is well reproduced when considering the following values for the linear cavity anisotropies: $\gamma_a = -0.7$ and $\gamma_p = 25$. The continuation results are displayed in figure 3 where we find a bifurcation sequence similar to the one for type II PS. However a chaotic region appears to be much larger and the periodic solution born on the Y-LP is stable only at very high injection current (orange line on figure 3). As shown in figure 3-(b) (the thick green line), the destabilization of the EP states leads the system to self-pulsing dynamics at the relaxation oscillation frequency F_{RO}. For higher current we only find complex nonlinear dynamics; a typical optical spectrum is given in figure 4. We find a two-mode emission, one on each linear polarization, with sidebands at F_{RO}; the splitting frequency between the two modes is given by the frequency of the unstable periodic solution born on Y-LP (orange line on figure 3). A similar optical spectrum is reported in figure 6 of Ref. [4] where the splitting frequency of the two-modes is referred to as the "effective birefringence".

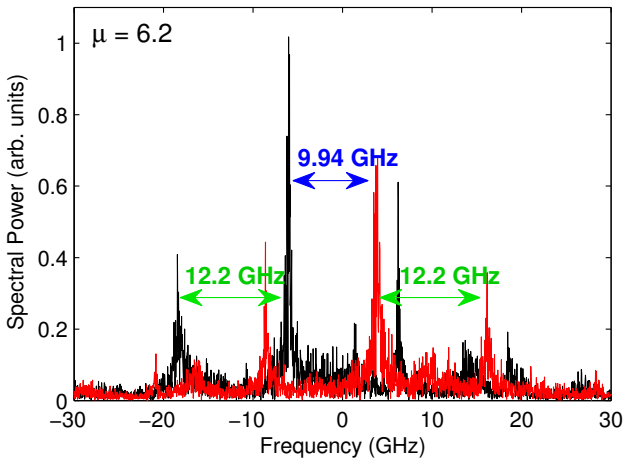

Figure 4: (color online) Optical spectrum for $\mu \sim 6.2$ for the same parameters as in figure 3. We find a two-mode emission: the frequency splitting between the two mode is given by the unstable periodic solution born on Y-LP branch $F = 9.94\ GHz$. We also find sidebands at the relaxation oscillation frequency $F_{RO} = 12.2\ GHz$.

5. Conclusions

In summary, the use of advanced continuation techniques allow us to follow for the first time the self-pulsating dynamics and secondary bifurcations leading to polarization chaos in free-running VCSELs. The frequency of the self-pulsating dynamics can be either close to the birefringence frequency or to the laser relaxation oscillation frequency, depending on the values of the linear cavity anisotropies. This theoretical work reconciles two apparently contradicting experiments [3, 4].

Acknowledgments

The authors acknowledge the support of CR Lorraine, FWO Vlaanderen and the Interuniversity Attraction Poles program of the Belgian Science Policy Office, under grant IAP P7-35 photonics@be.

References

[1] K.D. Choquette *et al.*, "Temperature dependence of gain-guided vertical-cavity surface emitting laser polarization," *Appl. Phys. Lett.*, vol.64, pp.2062–2064, 1994.

[2] M.B. Willemsen *et al.*, "Polarization switching of a vertical-cavity surface-emitting laser as a Kramers hopping problem," *Phys. Rev. Lett.*, vol.82, pp.4815–4818, 1999.

[3] M. Sondermann *et al.*, "Experimental and theoretical investigations of elliptically polarized dynamical transition states in the polarization switching of vertical-cavity surface-emitting lasers," *Optics Commun.*, vol.235, pp.421–434, 2004.

[4] L. Olejniczak *et al.*, "Polarization switching and polarization mode hopping in quantum dot vertical-cavity surface-emitting lasers," *Opt. Express*, vol.19, pp.2476–2484, 2011.

[5] M. San Miguel *et al.*, "Light polarization dynamics in surface-emitting semiconductor lasers," *Phys. Rev. A*, vol.52, pp.1728–1739, 1995.

[6] T. Erneux *et al.*, "Two-variable reduction of the San Miguel Feng Moloney model for vertical-cavity surface-emitting lasers," *Phys. Rev. A*, vol.59, pp.4660–4667, 1999.

[7] F. Prati *et al.*, "Analysis of elliptically polarized states in vertical-cavity surface-emitting lasers," *Phys. Rev. A*, vol.69, pp.033810, 2004.